GEOLOGICAL SURVEY OF CANADA
OPEN FILE 7453

Coupling between Power Systems and Pipelines during Geomagnetic Disturbances

L. Trichtchenko and D.H. Boteler

2013

Natural Resources Canada | Ressources naturelles Canada

Canada

GEOLOGICAL SURVEY OF CANADA
OPEN FILE 7453

Coupling between Power Systems and Pipelines during Geomagnetic Disturbances

L. Trichtchenko and D.H. Boteler

2013

doi:10.4095/292842

This publication is available for free download through GEOSCAN (http://geoscan.ess.nrcan.gc.ca/).

Recommended citation
Trichtchenko, L. and Boteler D.H., 2013. Coupling between Power Systems and Pipelines during Geomagnetic Disturbances; Geological Survey of Canada, Open File 7453, 37 p. doi: 10.4095/292842

Publications in this series have not been edited; they are released as submitted by the author.

SUMMARY

Design and operation of pipeline cathodic protection system for preventing pipeline steel corrosion as well as safety of crew during pipeline work need to take into account many factors. One of them is electromagnetic induction into a pipeline from the nearby power transmission lines.

The aim of the project is to examine the effects of electromagnetic induction from transmission line currents which includes not only 60 Hz currents, but also higher harmonics. These harmonics are produced by different technological and natural causes including geomagnetic storms.

The results of the modelling show that fundamental and third harmonic produce equal amplitude of pipe-to-soil potential and current in the nearby pipeline. The simplified approach used in this "pilot" study clearly demonstrates the need for more substantial work with realistic pipeline and power lines network modelling as well as field measurements for model validation.

CONTENTS

1. Introduction 4

2. Harmonic currents in power systems 6
2.1. Cause of harmonic currents 6
2.2. Currents in the power line phase conductors 7

3. Electric fields at the Earth surface produced by the currents in the power lines 9
3.1. Electric field calculations for a line current 9
3.2. Surface Impedance for a Layered Earth model 10

4. Pipeline response to harmonic currents in power line 12
4.1. Network model of a pipeline 12
4.2. Frequency-dependent pipeline parameters 13

5. Effects of harmonics on pipeline cathodic protection 18
5.1. Spectrum of harmonic currents 18
5.2. Ground electric field produced by each harmonic 18
5.3. Harmonic Pipe-to soil potential and currents in pipeline 21

6. Conclusions 24

7. Appendix 25
7.1 Fortran code to calculate geoelectric field 25
7.2 Fortran code to calculate PSP variations and current in pipeline 28

8. References 35

1. Introduction

Disturbances of the geomagnetic field produced by space weather events cause variable geoelectric field at Earth's surface which drive electric currents ("geomagnetically induced" currents, GIC) in long conductors, such as power systems and pipelines. These "primary" GIC produce a variety of effects on both ground systems which were described in many papers, such as Molinksi (2002), Gummow (2002) and Trichtchenko and Boteler (2003). One of the consequences of the increased GIC in power system is the generation of harmonic currents due to saturation of transformers. These high frequency harmonic currents (N·60 Hz, where N is an integer number) are capable of inducing "secondary" currents in adjacent pipelines (Figure 1). This report is concerned with the described aspect of "secondary" geomagnetic effects on pipeline operations, which has previously been overlooked.

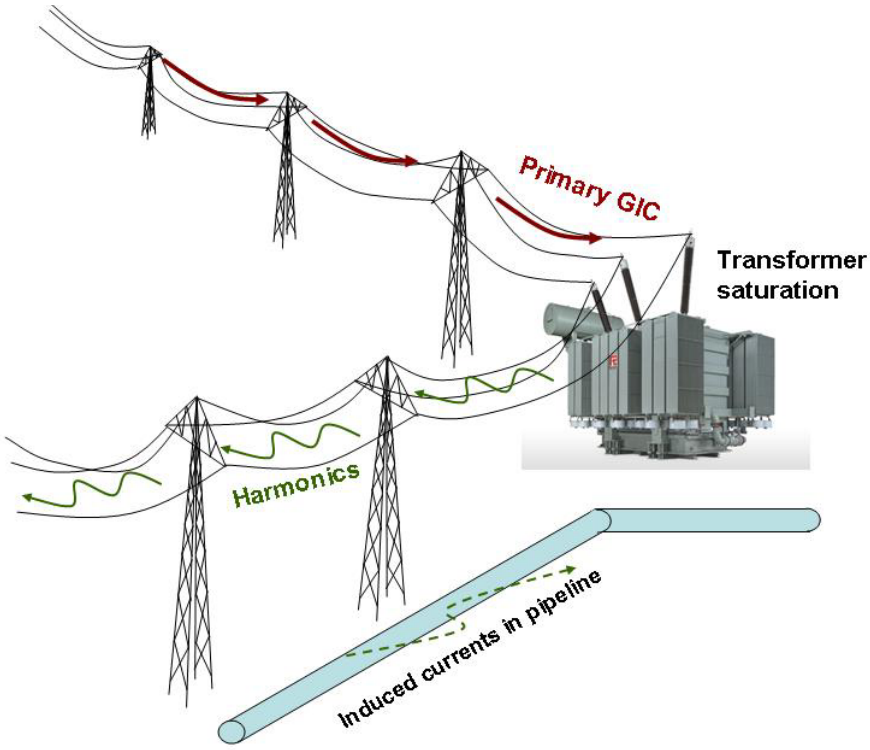

Figure 1. GIC in power systems cause transformer saturation, producing harmonic currents in power lines and induced currents in pipelines

The described process starts with GIC flowing through power transformers where the quasi-dc GIC creates an extra magnetic field in the transformer core. The resulting non-linear response of the transformer creates a distorted AC waveform that has a high content of harmonics.

Where pipelines share the same right-of-way with a power line, there is considerable electromagnetic coupling between the power line and the pipeline. There has been significant work on this issue (Taflove and Dabkowski, 1979; Dabkowski, 1999; Gummow et al, 1999), which has been almost exclusively concentrated on 60 Hz induction in pipelines. However, harmonics have also been observed in pipelines (Boteler et al. 2010; Boteler et al, 2013) and raised concerns about their contribution to the safe pipeline operation.

The results presented in this report are concerned with the impact of power system harmonics on pipe-to-soil potentials (PSP) and currents in pipelines sharing the same right-of-way with a power line. The report describes physical processes following the logic presented in Fig. 2.

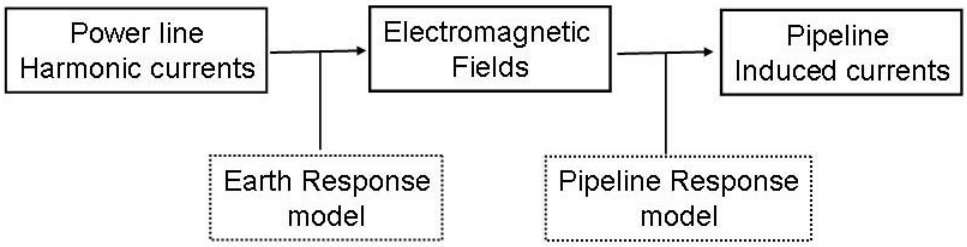

Figure 2. Logic of the steps towards evaluation of the pipeline response to harmonic currents in power grids

Part 1 of the report describes the source and characteristics of the harmonic currents produced in power systems by GIC causing saturation of power transformers. The magnetic and electric fields produced by each harmonic at the location of the pipeline is calculated using the complex image method to account for the effects of induced currents in the Earth, as described in the Part 2.

Part 3 shows how to set up the numerical model of the pipeline that includes frequency-dependent electromagnetic parameters of the pipeline circuit elements necessary for modelling the currents in the pipeline and the pipe-to-soil potential (PSP) produced by different harmonics.

Finally, in Part 4 all these components are combined to show the pipeline response resulting from the GIC-produced harmonics in the power system.

2. Harmonics in Power Systems

2.1. Cause of Harmonics

Geomagnetically induced currents (GIC) in power systems flow to ground through the windings of power transformers where these extra currents create partial saturation of the transformer core. This can be illustrated by considering the hysteresis curve of Figure 3.

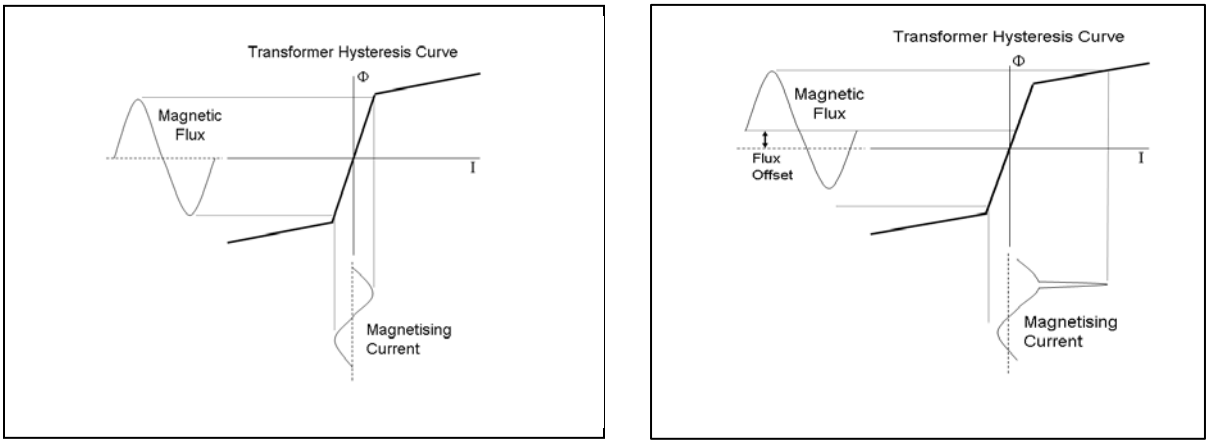

a) b)

Figure 3. Transformer hysteresis curves representing two cases:
a) during normal operation;
b) flux offset created by GIC shifts the operating regime into saturation

In normal operation (Fig. 3a), the sinusoidal magnetic flux is symmetrical about zeroand is confined to the linear operating regime of the transformer. Accordingly, the flux produces a sinusoidal magnetising current which is symmetrical about zero.

When GIC flows through the neutral of transformer, the extra magnetic field produced shifts the operating point so that the peak of the AC cycle goes past the knee in the hysteresis curve producing a spike in the magnetising current which leads to the harmonics in this current. These AC harmonic currents (although much smaller than load current) flow along the transmission lines and create magnetic fields producing inductive coupling with nearby conducting lines (pipelines).

Fourier analysis of the distorted AC current waveform shows that, in addition to an increase in the fundamental (60Hz) component of the magnetising current, there are also components at the even and odd harmonics (120 Hz, 180 Hz etc.). Here the general formulas will be derived for the harmonic currents up to the third order.

2.2 Currents in the power line phase conductors

In three-phase operation, as used in most power systems, each of the three conductors in a transmission line is delivering the current from one phase of the three-phase generator. These three currents have the same amplitudes but the phases are 120 degrees apart (Equation (1)). Thus, in a well-balanced system the separate phase currents should add up to zero at the transformer neutral point.
The currents are expressed as follows:

$$\begin{aligned} i_a &= I_{1a}\cos(\omega t) \\ i_b &= I_{1b}\cos(\omega t + 240) \\ i_c &= I_{1c}\cos(\omega t + 120) \end{aligned} \qquad (1)$$

where i_a, i_b, i_c, are the currents in each of three phase lines for the "fundamental " (i.e. 60Hz) frequency at each moment t; I_{1a},I_{1b} and I_{1c} are their amplitudes, and ω is angular frequency. The *a, b, c* subscripts are related to the sequence of the currents from the rotating machine as illustrated in Fig. 4a (so-called "positive sequence").

When there is an imbalance in the system, these three phase currents do not add up to zero. In power system engineering this imbalanced current is usually represented as a combination of three specifically defined configurations of balanced "sequence components". These are the positive sequence, as for the normal operations, negative and zero sequences, as shown in Figure 4.

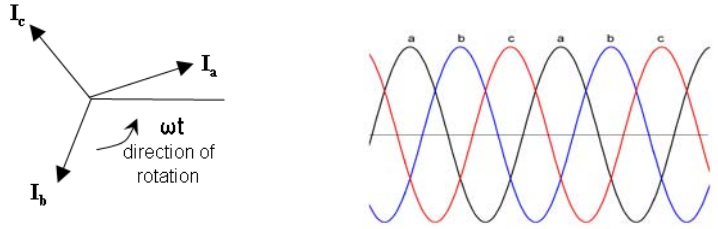

a) positive sequence (order of maxima occurrence is abc)

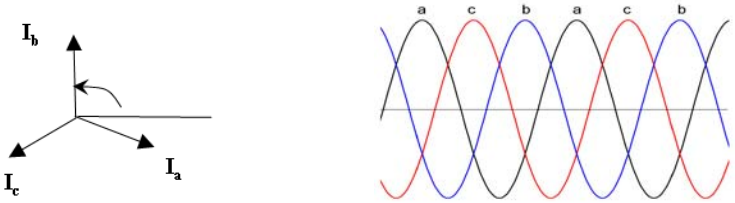

b) negative sequence (order of maxima occurrence is acb)

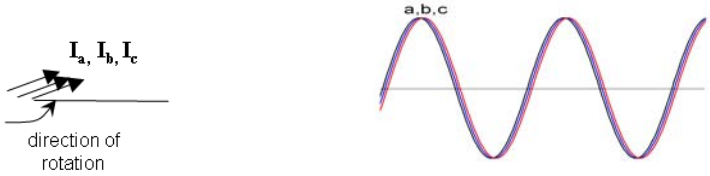

c) zero sequence (simultaneous maxima occurrence)

Figure 4. Vector (left) and time-variation (right) schemes of the phase currents for three sequences used to present any unbalanced case: a) positive, b) negative, and c) zero

The concept of "sequence components" was first proposed in 1895 and later the mathematical analysis was done in 1912 and 1915 and since then it has been widely used in power engineering (e.g. Wagner and Evans, 1933; Blackburn, 1993 and references therein).

When higher harmonics are presented, currents in each phase (a, b and c) can be represented as Fourier series, i.e.

$$
\begin{aligned}
i_a &= I_{1a}\cos(\omega t) + I_{2a}\cos(2\omega t) + I_{3a}\cos(3\omega t) + \ldots. \\
i_b &= I_{1b}\cos(\omega t + 240) + I_{2b}\cos(2(\omega t + 240)) + I_{3b}\cos(3(\omega t + 240)) + \ldots \\
i_c &= I_{1c}\cos(\omega t + 120) + I_{2c}\cos(2(\omega t + 120)) + I_{3c}\cos(3(\omega t + 120)) + \ldots
\end{aligned}
$$

where index 1 is for fundamental (60Hz), 2 for the second harmonic (120 Hz) and 3 for the third harmonic (180 Hz).
After re-arrangements and subtraction of any multiple of 360 in *b* and *c* phases, we have

$$
\begin{aligned}
i_a &= I_{1a}\cos(\omega t) + I_{2a}\cos(2\omega t) + I_{3a}\cos(3\omega t) + \ldots \\
i_b &= I_{1b}\cos(\omega t + 240) + I_{2b}\cos(2\omega t + 120)) + I_{3b}\cos(3\omega t) + \ldots \qquad (2) \\
i_c &= I_{1c}\cos(\omega t + 120) + I_{2c}\cos(2\omega t + 240) + I_{3c}\cos(3\omega t) + \ldots
\end{aligned}
$$

Thus, the harmonic components in each phase conductor *a, b* and *c* have phase relations as shown in Table 1.

Table 1. Phase relations of harmonics on a 3-phase system

Harmonic	Frequency	Phase of i_a	Phase of i_b	Phase of i_c	Phase Sequence
1(fundamental)	60Hz	0	240	120	Positive
2	120Hz	0	120	240	Negative
3	180Hz	0	0	0	Zero
4	240Hz	0	240	120	Positive
5	300Hz	0	120	240	Negative
6	360Hz	0	0	0	Zero

From these equations it follows that summations of the harmonic currents from all three phases reduces any frequency except multiple of 3, because the 3-rd harmonic has zero phase sequence. Therefore, currents induced in the pipeline might have significant response to the third harmonic.

3. Electric Fields at the Earth surface produced by the currents in the power lines

The harmonically-varying currents in the power lines create a changing magnetic field and electric fields in the surrounding media and at the pipeline location. Assuming the amplitudes of fundamental and harmonic currents are monitored in the power grid, our next task (following the logic presented in Fig. 2) is to find the electric field in the earth produced by these currents.

The electric field E produced at the Earth's surface by an external source satisfies the diffusion equation in the form:

$$\nabla^2 E = i\omega\mu\sigma E \qquad (3)$$

where $i = \sqrt{-1}$, ω is angular frequency of the source, μ is magnetic permeability and σ is conductivity of the media.

3.1. Electric field calculations for a line current source

The geomagnetic coordinate system, i.e. X-axis is directed northward, Y-axis is directed eastward and Z-axis downward (Fig. 5), with line current I located at the height of –h (i.e. current in the overhead power line) and is directed along Y-coordinate has been used.

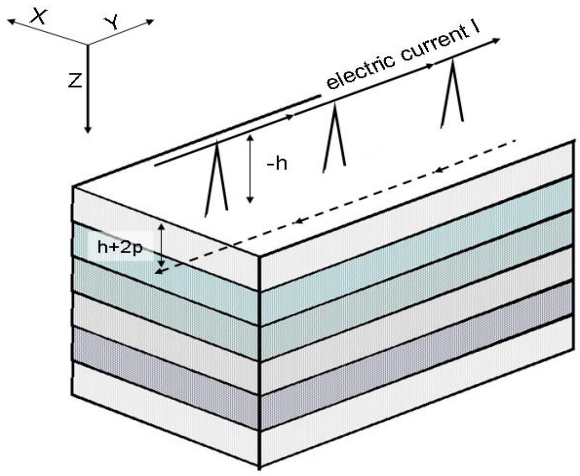

Figure 5. Schematic representation of a current in the overhead wire (at a height –h) and image current in the Earth (at a depth h+2p)

The solution of the equation (3) at the surface of the Earth can be written as (Hermance and Peltier, 1970; Wait, 1992; Boteler and Pirjola, 1998)

$$E_y = -I\frac{i\omega\mu_0}{2\pi}\int_0^\infty (1 - R(\nu))\, e^{-h\nu}\, \frac{\cos\nu x}{\nu}\, d\nu \qquad (4)$$

where R is the reflection coefficient representing properties of the conducting earth, ν is the integration variable called "wavenumber" representing the geometrical properties of the

cylindrical electromagnetic wave created by a line current. The result of integration will be independent of this variable.
The reflection coefficient can be expressed as

$$R = \frac{i\omega\mu_0 / Z - \nu}{i\omega\mu_0 / Z + \nu}, \tag{5}$$

where Z is the surface impedance (see the paragraph 3.2 below).

To solve (4) analytically, the refelection coefficient can be approximated as (Boteler and Pirjola, 1998)

$$R = \frac{1/p - \nu}{1/p + \nu} \approx \exp(-2p\nu) \tag{6}$$

where

$$p = \frac{Z}{i\omega\mu_0} \tag{7}$$

Substituting for R in equation (4) gives the expression for the electric fields:

$$E_y = -I\frac{i\omega\mu_0}{2\pi}\ln\frac{\sqrt{(h+2p)^2 + x^2}}{\sqrt{h^2 + x^2}} \tag{8}$$

This shows that the electric field at the surface of the Earth can be thought of as the sum of an external part (produced by a line source) and an internal part (produced by an image current at a "complex" depth $h+2p$).

Equation (4) or in more simple form Eq. (8) together with either (5) or (6) and (7) can be used to calculate the approximate values of electric fields at the Earth's surface at location x from the vertical projection of phase current I to the earth surface.

3.2. Surface Impedance for a Layered Earth model

For the "layered" earth model (Figure 6) , the unknown impedance Z can be found from general formulas of impedance at the surface of any layer n (where n=1 is the surface of the Earth and n=N is the last layer before the uniform half-space) by applying the recursion relation (Weaver, 1994).

$$Z_n = i\omega\mu\left(\frac{1 - r_n e^{-2k_n d_n}}{k_n(1 + r_n e^{-2k_n d_n})}\right) \tag{9}$$

where d_n and k_n are thickness and propagation constant of layer n, with propagation constant depending on the layer's conductivity as: $k_n = \sqrt{i\omega\mu_0\sigma_n}$ and r_n are the reflection coefficients at each layer boundary (except the last layer N)

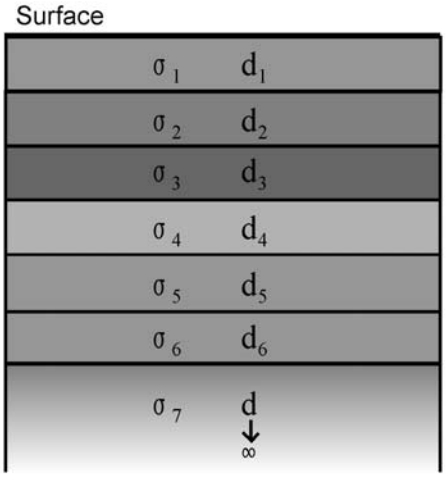

Figure 6. Schematic representation of the layered earth model with conductivities σ_n and thicknesses d_n of each layer.

The reflection coefficients are defined as:

$$r_n = \frac{1 - k_n \dfrac{Z_{n+1}}{i\omega\mu}}{1 + k_n \dfrac{Z_{n+1}}{i\omega\mu}} \tag{10}$$

and for the last layer

$$Z_N = \frac{i\omega\mu}{k_N} \tag{11}$$

4. Pipeline Response to Harmonics

4.1. Network model of a pipeline

The electric field induced in the pipeline produces variations in the pipe-to-soil potential (PSP). The exact PSP produced depends on the electrical characteristics of the pipeline. This can be modelled using transmission line theory (Taflove and Dabkowski, 1979). The starting point is the approximation of pipeline network by the series of uniform sections with the geoelectric field *E* in each section (Figure 7).

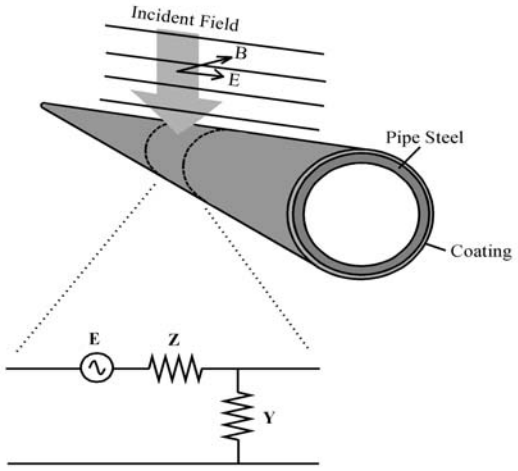

Figure 7. Schematic representation of the uniform element of a pipeline network.

The voltage and current along the line are given by

$$\frac{dV}{dx} + ZI = E \tag{11}$$

and

$$\frac{dI}{dx} + YV = 0 \tag{12}$$

from which differentiation and substitution lead to the equations

$$\frac{d^2V}{dx^2} - \gamma^2 V = \frac{dE}{dx} \tag{13}$$

and

$$\frac{d^2I}{dx^2} - \gamma^2 I = -YE \tag{14}$$

where Z and Y are the series impedance along the pipeline and the parallel admittance of the pipeline coating. These are used to determine the characteristic impedance, Z_0, and the propagation constant, γ, given by

$$Z_0 = \sqrt{\frac{Z}{Y}} \qquad \gamma = \sqrt{ZY}$$

If the electric field is assumed to be uniform within a section of pipeline, $dE/dx = 0$ and equation (13) becomes

$$\frac{d^2V}{dx^2} - \gamma^2 V = 0 \tag{15}$$

Equations (14) and (15) have solutions of the form

$$V = Ae^{\gamma x} + Be^{-\gamma x} \tag{16}$$

and

$$I = \frac{E}{\gamma Z_0} - \frac{A}{Z_0}e^{\gamma x} + \frac{B}{Z_0}e^{-\gamma x} \tag{17}$$

where A and B can be found from conditions at the ends of the pipeline.
At x=0 equation (16) gives

$$V_i = A + B \tag{18}$$

While at the end of the section, $x = L$, equation (16) gives

$$V_k = Ae^{\gamma L} + Be^{-\gamma L} \tag{19}$$

Combining these two equations gives

$$A = \frac{V_k - V_i e^{-\gamma L}}{e^{\gamma L} - e^{-\gamma L}} \tag{20}$$

and

$$B = \frac{V_i e^{\gamma L} - V_k}{e^{\gamma L} - e^{-\gamma L}} \tag{21}$$

Substituting for A and B in equation (16) for voltage gives

$$V = \left(\frac{V_k e^{\gamma L} - V_i}{e^{\gamma L} - e^{-\gamma L}}\right)e^{-\gamma(L-x)} + \left(\frac{V_i e^{\gamma L} - V_k}{e^{\gamma L} - e^{-\gamma L}}\right)e^{-\gamma x} \tag{22}$$

Similarly substituting for A and B in equation (17) for current gives

$$I = -\frac{1}{Z_0}\left(\frac{V_k e^{\gamma L} - V_i}{e^{\gamma L} - e^{-\gamma L}}\right)e^{-\gamma(L-x)} + \frac{1}{Z_0}\left(\frac{V_i e^{\gamma L} - V_k}{e^{\gamma L} - e^{-\gamma L}}\right)e^{-\gamma x} + \frac{E}{\gamma Z_0} \tag{23}$$

This represents the variation of voltage and current within a uniform pipeline section. Combining these sections as Thevenin equivalent circuits (Taflove and Dabkovski, 1979) or pi-circuits (Boteler, 2013), induced currents and voltages can be calculated.

4.2. Frequency dependent pipeline parameters

The key characteristics of the pipeline are the series impedance, Z, along the pipeline and the parallel admittance, Y, of the pipeline coating. Assuming the pipeline has a simple multilayered structure as shown in Figure 8 with layers 1,2,3,4, are soil, coating, steel and

gas (oil) respectively with their electromagnetic parameters, σ, conductivity, ε, dielectric permittivity and μ, relative magnetic permeability.

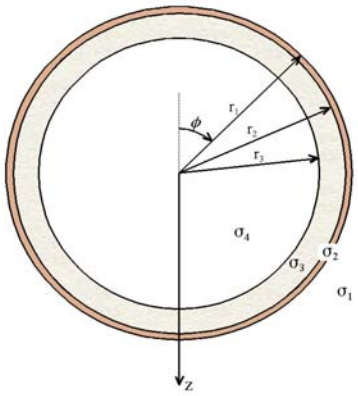

Figure 8. Schematic representation of the pipeline as a layered cylinder

The response of the pipeline to the external electoromagnetic wave (with electric field parallel to the pipeline axis) can be modelled as diffusion equation in cylindrical coordinate system. The exact solution of this equation with appropriate boundary conditions is presented by Trichtchenko and Boteler (2001). Example of the variations of electric field outside and inside the pipeline layers (normalised to the electric field in the absence of the pipeline) for 60 Hz frequency is shown in Figure 9.

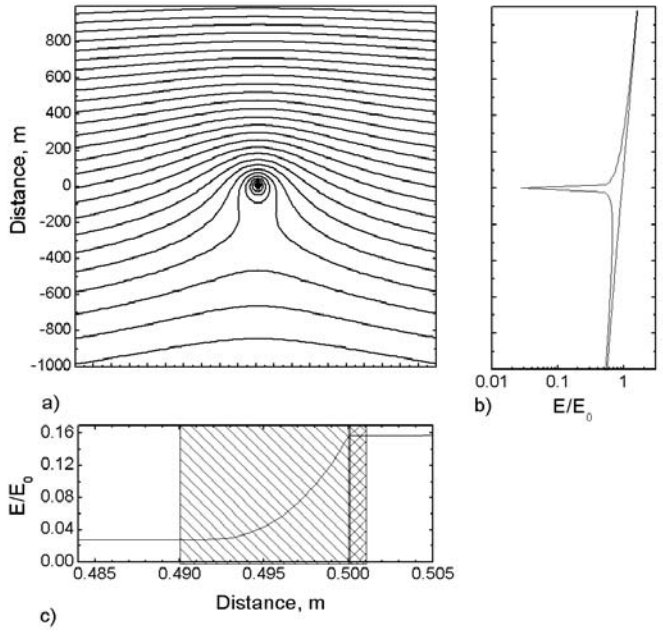

Figure 9. Example of the modelling of the layered cylinder. The normalized absolute value of the electric field, *f*=60 Hz,

a) contour lines; b) values along cross section at X=0 and X=1000m

c) magnified view across the pipeline wall

Thus, for frequencies 60 Hz and higher the electric field does not uniformly penetrate the steel and the depth of penetration decreases with increasing frequency. Therefore the impedance along the pipeline is frequency dependent.

Total impedance is the sum of the external and internal impedances.

$$Z_{total} = Z_{ext} + Z_{\text{int}} \tag{24}$$

In this formula the total impedance represents the ratio of the current in the pipeline steel to the electric field in the absence of the pipeline (i.e. induced in the ground).

For the external impedance, the simple representation, so called Dubanton equation (Gary, 1976; Deri et al, 1981) exists which is a good approximation of the Carson (1926) formulas. This simple representation is used also by Dabkowski (1999) for calculations of the longitudinal electric field in pipelines produced by the power line interference.

$$Z_{ext} = \frac{i\omega\mu_1}{2\pi} \ln \frac{2}{k_1 R_2} \tag{25}$$

where index 1 is referred to the surrounding medium (soil), and R_2 is the outer radius of the pipeline steel .

For the internal impedance (with external return), which represents the AC-resistance of the pipeline steel, we use approximation given by Sunde (1968), his equation (1.111).

$$Z_{\text{int}} = \frac{2\gamma\delta\rho}{[\exp(\gamma\delta) - \exp(-\gamma\delta)]} = \frac{\gamma\delta\rho}{sh(\gamma\delta)} \tag{26}$$

where

$$\gamma = \sqrt{\frac{i\omega\mu_3\rho}{2\pi\delta\, R_{av}}} \tag{27}$$

$R_{av}=(R_2+R_3)/2$ is mean radius of the pipeline steel layer, δ is thickness of the steel and ρ is DC-resistance per unit length, μ_3 is steel permeability, and $\rho = 1/(\pi\sigma_3(R_2^2 - R_3^2))$ where index 3 refers to the internal surface of the pipeline steel layer, index 2 to the external surface of the steel layer and index 1 to the external radius of the pipeline together with coating.

Verification of the above expressions for the frequency dependent impedances has been carried out by Trichtchenko et al, (2004) and is presented in Figure 10.

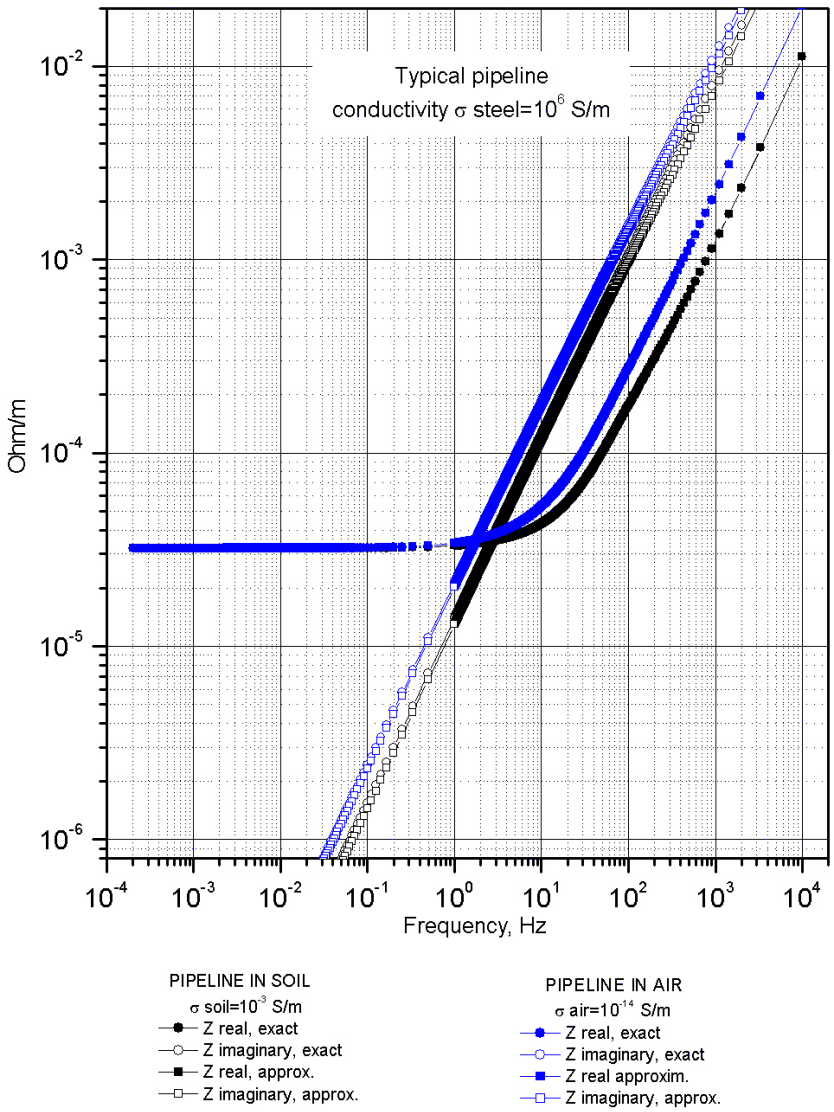

Figure 10. Comparisons of the impedances calculated by exact method (Trichtchenko et al, 2004) and analytical approximations (equations 24-26) for pipeline in soil and in air.

To complete the derivation of the frequency-dependent parameters of the pipeline,we also need to know the admittance ***Y*** through the pipeline coating to ground. This is a complex value and includes both the capacitance ***C*** between pipeline steel as one plate and surface of the earth as another as well as conductance through the coating. Therefore, the admittance is

$$Y = Q + i\omega C \qquad (28)$$

where $Q=2\pi\xi_2 R_1$ with R_1 is external radius of pipeline (with coating), ξ_2 is coating conductance (S/m^2), and $C=2\pi\varepsilon_2/ln(R_1/R_2)$, ε_2 is coating permittivity.

The variation of the admittance with frequency is shown below in Figure 11.

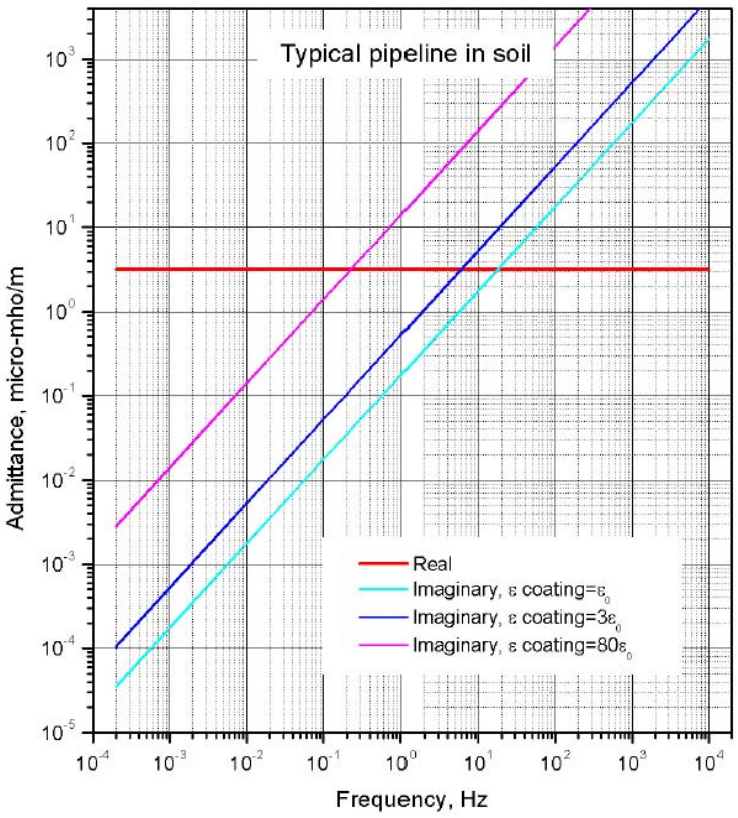

Figure 11. Real and imaginary parts of a complex admittance of pipeline for 3 cases of different coating permittivities and external radius 0.457 m, internal radius is 0.448 m, coating conductance is $2.\cdot10^{-5}$ S/m^2, thickness 0.00025 m

5. Effects of harmonics on pipeline cathodic protection

The previous sections have shown how the frequency and phase relations of harmonic currents affect the electric field induced in the pipeline; how the complex image method can be used to account for the effects of induced currents in the Earth; and how the pipeline response to a specified electric field can be modelled using DSTL theory and the NPM method. Now we combine all these parts to calculate the PSP produced in a pipeline by a realistic set of harmonic currents flowing in an adjacent power line.

The Steps to calculate the currents and voltages in the pipeline induced by the harmonics are:

i) Specify a spectrum of harmonic currents
ii) Calculate the electric fields produced by each harmonic
iii) Calculate the PSP produced by each harmonic electric field

5.1. Spectrum of harmonic currents

In our example only fundamental, second and third harmonics will be discussed. The fundamental corresponds to a positive sequence, second to a negative sequence, third to a zero sequence, i.e. by this example all three sequence configurations are covered.
Fundamental current is 1000A, second and third are 1%, which is 10A each (power engineer, personal communication, 2013).

5.2. Ground electric field produced by each harmonic

To illustrate the calculations of electric field produced by each harmonic at the Earth surface, consider the three-phase transmission line configuration as shown in Figure 12.
Electric field produced by each harmonic current can be presented as:
Fundamental (positive sequence):

$$E_1 = I_1\left[(E_{1aL} + E_{1aR}) + (E_{1bL} + E_{1bR})\cos(240^o) + (E_{1cL} + E_{1cR})\cos(120^o)\right] \qquad (29)$$

Second Harmonic (negative sequence):

$$E_2 = I_2\left[(E_{2aL} + E_{2aR}) + (E_{2bL} + E_{2bR})\cos(120^o) + (E_{2cL} + E_{2cR})\cos(240^o)\right] \qquad (30)$$

Third Harmonic (zero sequence):

$$E_3 = I_3\left[(E_{3aL} + E_{3aR}) + (E_{3bL} + E_{3bR}) + (E_{3cL} + E_{3cR})\right] \qquad (31)$$

where E_{1aL}, E_{1aR}, E_{2aL}, E_{2aR}, E_{3aL}, E_{3aR} are normalised electric fields (i.e. electric field per unit current) produced by the current in the phase *a* at the frequency of each harmonic (1,2 or 3) and by each conductor (left and right) respectively. Similar notations are used for normalised electric fields produced by phase *b* and phase *c*.

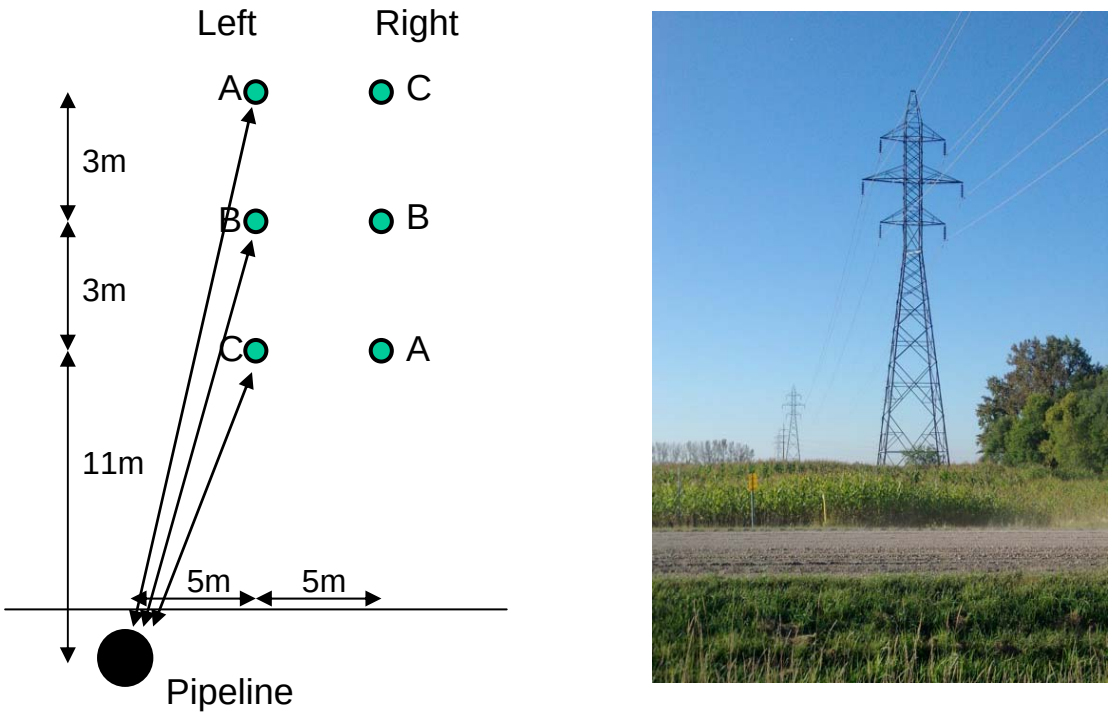

Figure 12. Arrangement of power line/pipeline used for calculations; a) Diagram showing distances from conductors to pipeline: b) Photo of the transmission line next to a pipeline (yellow marker)

The normalised electric fields at the earth surface produced by each separate line at each of three frequency can be found from (8), i.e.

$$E/I = -\frac{i\omega\mu_0}{2\pi}\ln\frac{\sqrt{(h+2p)^2+x^2}}{\sqrt{h^2+x^2}} \qquad (32)$$

where h is the height of each conductor above the surface, x is the horizontal distance from the conductor to pipeline location (as per Figure 4a) and $h+2p$ is the complex depth location of the image current with respect to the earth surface (Eq. (7)).

For our calculations the layered earth model has been chosen to have 11 layers and two different arrangements, such as
Case 1, "Resistive Earth" model with depths (in meters) as:
100, 1000, 10000, 14000, 75000, 100000, 160000, 110000, 150000, 230000, 10^9
and conductivities (in 1/Ohm-m) as:
0.01, 0.0077, 0.0002, 0.008, 0.0033, 0.0063, 0.0346, 0.1258, 0.4168, 1.122, 2.0892

Case 2, the hypothetical layered earth with top sea water layer with same depths of layers but conductivities (in 1/Ohm-m) as:

1.00, 0.0077, 0.0002, 0.008, 0.0033, 0.0063, 0.0346, 0.1258, 0.4168, 1.122, 2.0892

Results of these calculations are presented in Table 2 (case 1) and Table 3 (case 2) and Figures 13 and 14.

Table 2. results of electric field calculations for Case 1 (Resistive Earth) model

Freq	Surface Impedance (amplitude)	Surface Impedance (phase)	Electric Field (amplitude)	Electric Field (phase)
60 Hz	0.222 Ohm	42.811 degrees	4.8910^{-3} V/m	-90 degrees
120 Hz	0.329 Ohm	44.008 degrees	$9.779*10^{-5}$ V/m	-90 degrees
180 Hz	0.404 Ohm	43.163 degrees	$4.998*10^{-2}$ V/m	77.46 degrees

Table 3. results of electric field calculations for Case 2 (Seawater top) model

Freq	Surface Impedance (amplitude)	Surface Impedance (phase)	Electric Field (amplitude)	Electric Field (phase)
60 Hz	$2.017 *10^{-2}$ Ohm	44.758 degrees	$4.911*10^{-3}$ V/m	-90 degrees
120 Hz	$3.055*10^{-2}$ Ohm	46.151 degrees	$9.855*10^{-5}$ V/m	90 degrees
180 Hz	$3.788*10^{-2}$ Ohm	45.379 degrees	$2.072*10^{-2}$ V/m	66.122 degrees

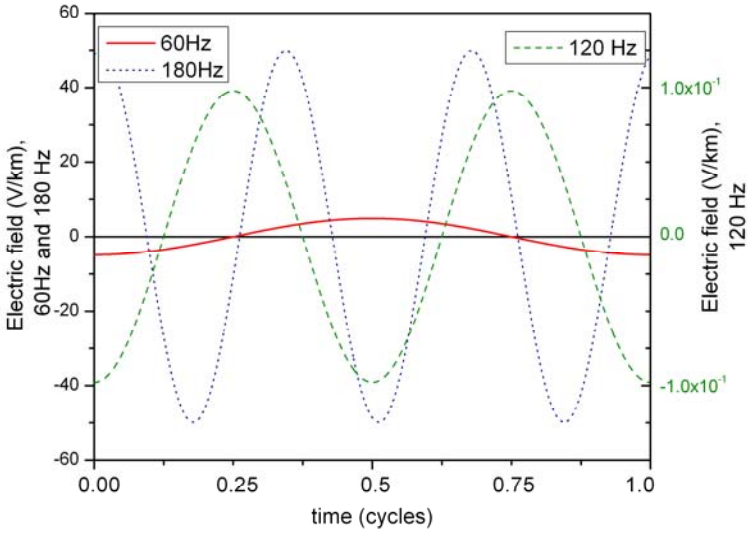

Figure 13. Results of the electric field calculations for Case 1, Resistive Earth. The currents in power transmission lines are set to 1000A (60Hz), 10A (120Hz), 10A (180Hz). Note the scales for 2nd harmonic–associated electric field (green lines) are different (shown in green).

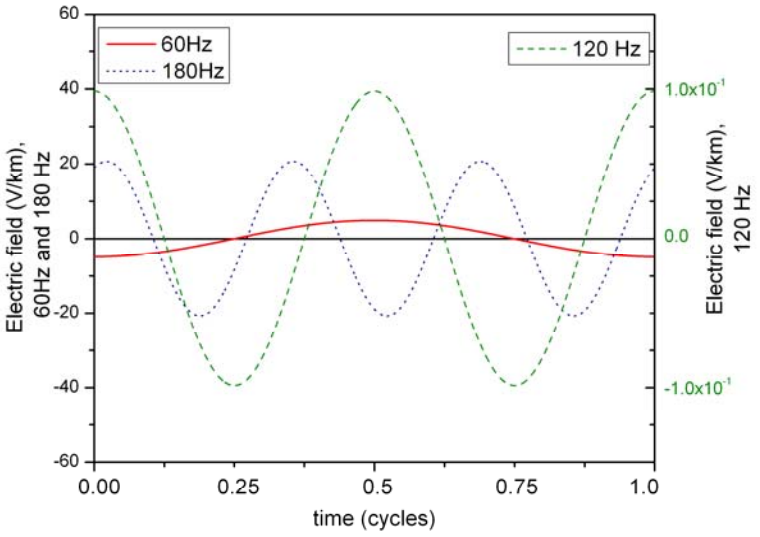

Figure 14. Results of the electric field calculations for Case 2 (Seawater top) layered earth models. The currents in power transmission lines are set to 1000A (60Hz), 10A (120Hz), 10A (180Hz). Note the scales for 2nd harmonic–associated electric field (green lines) are different.

5.3. Harmonic Pipe-to soil potential and currents in pipeline

To illustrate the calculations of PSP and currents produced by harmonics, an example pipeline with the following parameters was used.
Uniform pipeline section (no bends) with the length of 450 km is running along the power line with terminating impedances of 0.1 Ohms at both ends of the pipeline. The low values of terminating impedances are chosen in order to anticipate possible continuations of pipeline at both ends. The pipe-to soil potential and current are calculated at the distance of the 185 km from the beginning of the pipeline.

Table 4, Geometric and electromagnetic characteristics of pipeline

Dimensions of pipeline		Electromagnetic Properties	
External Radius	0.457 m	Steel Conductivity	$5*10^6$ S/m
Internal Radius	0.448 m	Coating Conductance	$20*10^{-6}$ S/m^2
Coating Thickness	0.00025 m	Steel Permeability	150 (relative)
		Coating Permittivity	3 (relative)

Table 5, Pipeline inmedances and admittances at 3 different frequencies

Freq Hz	Pipeline Impedance (real) Ohm/km	Pipeline Impedance (imaginary) Ohm/km	Coating Admittance (real) S/km	Coating Admittance (imag) S/km
60	0.089	0.572	0.0574	0.115
120	0.160	1.074	0.0574	0.230
180	0.229	1.554	0.0574	0.344

Variations of the pipe-to-soil potential and current along the pipeline for two cases surface impedance (or the layered earth models) are presented in the following figures.

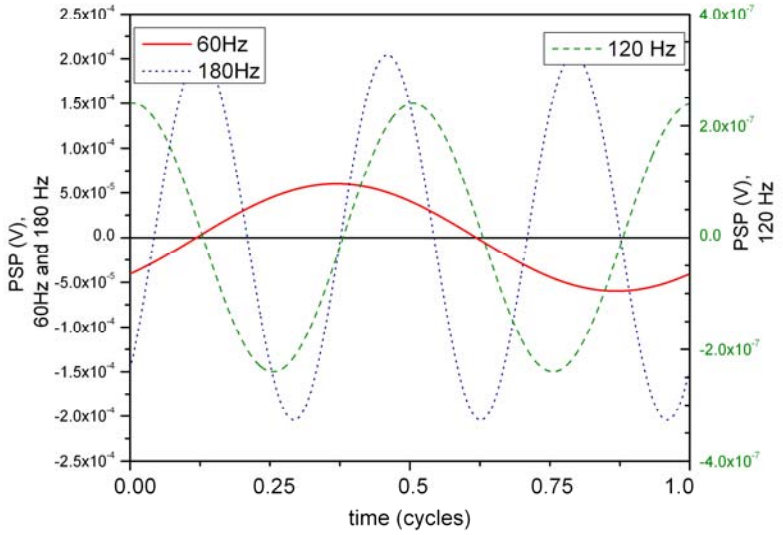

Figure 15 Variations of PSP at Km 185 due to harmonics with a resistive earth model (case 1). The currents in power transmission lines are set to 1000A (60Hz), 10A (120Hz), 10A (180Hz)

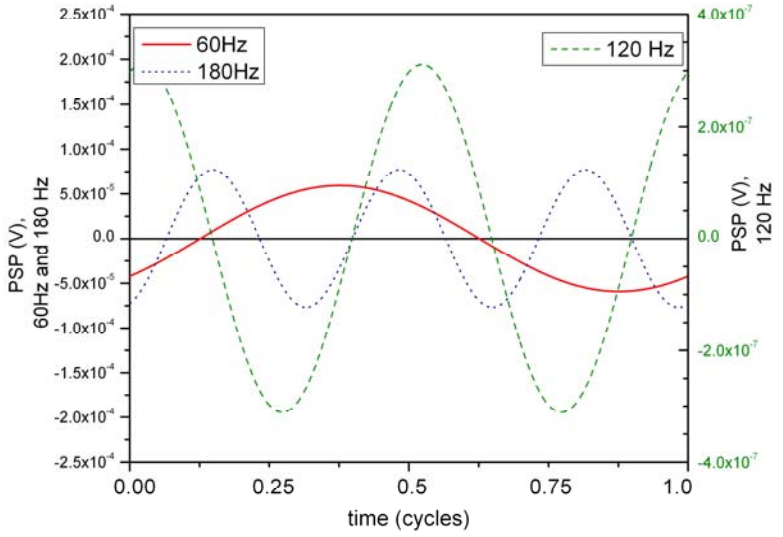

Figure 16. Variations of PSP at Km 185 due to harmonics with a top sea water model (case 2). The currents in power transmission lines are set to 1000A (60Hz), 10A (120Hz), 10A (180Hz)

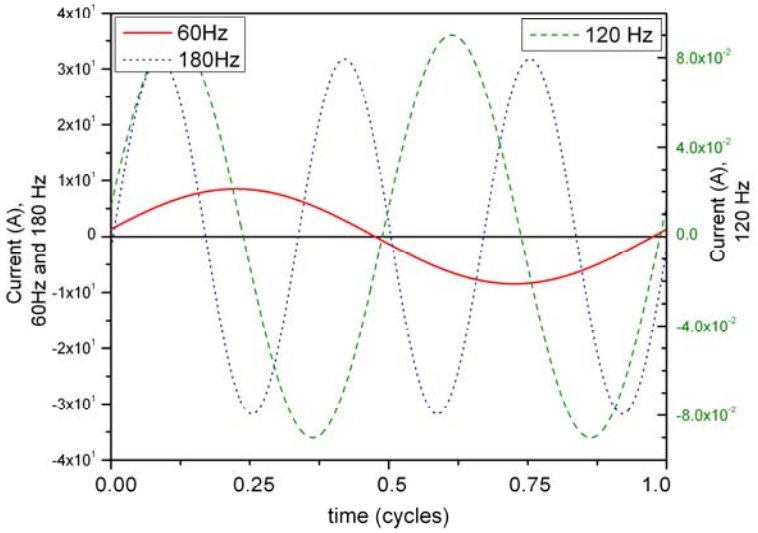

Figure 17 Variations of pipeline current due to harmonics with a resistive earth model (case 1). The currents in power transmission lines are set to 1000A (60Hz), 10A (120Hz), 10A (180Hz)

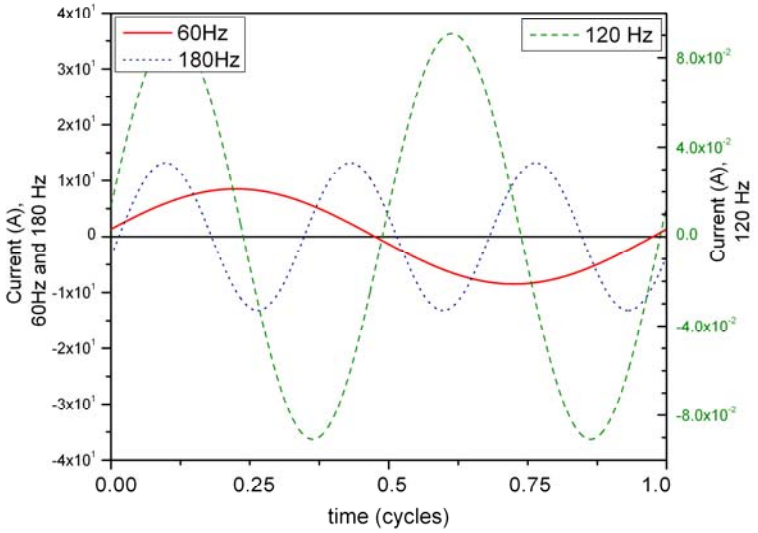

Figure 18. Variations of pipeline current due to harmonics with a top sea water model (case 2). The currents in power transmission lines are set to 1000A (60Hz), 10A (120Hz), 10A (180Hz)

6. Conclusions

This report examines the effects on pipelines from harmonic currents produced in power lines during geomagnetic disturbances. On 3-phase lines the different harmonics have different phase relations and are classified as ‘positive sequence’, ‘negative sequence’, and ‘zero sequence’.

The transmission line currents can be used with an earth conductivity model to calculate the electric fields produced at the locations of adjacent pipelines. Pipeline network modelling can then be used to determine the pipe-to-soil potential (PSP) variations and pipeline currents that are produced.

All these steps can be combined to calculate the PSP and pipeline currents produced by harmonic currents in a nearby power line.

The results show that PSP and current in pipeline due to the third harmonic can be higher than those due to the unbalanced fundamental frequency in case of the resistive top layer of the layered earth model and comparable with those induced by fundamental frequency if the top layer is conductive (sea water).

Further work is needed to validate the calculations by more experimental measurements in the field. As well, application to more realistic arrangements of pipeline and transmission line networks configurations needs to be examined

7. Appendix

7.1 FORTRAN Code 1

```
Calculation of electric field in the ground induced by power line harmonic currents
 Earth conductivity model as per Ontario 2013 report,
 ON1-zone 1 of the Ontario report (Case 1 of this report). ON2-top layer of Zone 1 changed
to sea water (1.0 Ohm-m), case 2 of this report
 Bottom layer has been changed to thickness of 1E9m
Ea,b,c-electric field produced by each phase,left and right sides of tower,normalised by
amplitude current,
P is skin-depth(dependent on freq), h and x are locations with respect to pipeline

      parameter  (npoint=3)    !number of harmonics (npoint=1 is 60 Hz)
      REAL dOn1(11),sigmaOn1(11),dOn2(11),sigmaOn2(11), Cur(npoint)
      REAL ZR(npoint),ZI(npoint),ZA(npoint), Zph(npoint), F(npoint)
      REAL AMPLE(npoint),Phase(npoint)
      COMPLEX cOn1(11),cOn2(11)
      COMPLEX Z(npoint),Z1(npoint),ZZ(npoint),E(npoint)
      Complex EaL(npoint), EbL(npoint), EcL(npoint), P(npoint)
      Complex EaR(npoint), EbR(npoint), EcR(npoint)

C Power Tower Arrangements in meters from pipeline
      XcL=5.
      XaL=5.
      XbL=5.
      HcL=11.
      HbL=14.
      HaL=17.

      XcR=10.
      XbR=10.
      XaR=10.
      HcR=17.
      HbR=14.
      HaR=11.
C currents for each harmonic
      Cur(1)=1000.
      Cur(2)=10.
      Cur(3)=10.

C Ontario model

      data dOn1/100.,1000.,10E3,14E3,75E3,100E3,160E3,110E3
     *  ,150E3,230E3,1E9/
      data sigmaOn1/0.01,0.0077,0.0002,0.008,0.0033,0.0063,0.0346,0.1258
     *  ,0.4168,1.122,2.0892/
```

```
C Ontario model with top water
      data dOn2/100.,1000.,10E3,14E3,75E3,100E3,160E3,110E3
      *,150E3,230E3,1E9/
      data sigmaOn2/1.,0.0077,0.0002,0.008,0.0033,0.0063,0.0346,0.1258
      *,0.4168,1.122,2.0892/

      NON=11
      PI=3.1415926
      TOPI=2.*PI
       U=4.*PI*1.e-7 ! magn perm of free space
       rnu=0. !wavenumber=0,plane wave model

       do I=1, npoint
       F(i)=FLOAT(i)*60.
       OMG=TOPI*F(i)
    call layered_Earth(sigmaON2,dON2,OMG,rnu,NON,cON2)
C       Z(I)=(0.,1.)*TOPI*F(i)*cQ(1) ! in m/s
      Z1(i)=(0.,1.)*TOPI*F(i)*cON2(1)*U  !in Ohm
      ZR(i)=REAL(Z1(i))
      ZI(i)=AIMAG(Z1(i)) ! not inverted
      ZZ(i)=CMPLX(ZR(i),ZI(I))
      ZA(i)=SQRT(ZR(i)*ZR(i)+ZI(i)*ZI(i))
      Zph(i)=ATAN(ZI(i)/ZR(i))*180./PI
      P(i)=ZZ(i)/(0.,1.)/OMG/U

C Calculations of the E of each phase normalised by currents/change to function

      EaL(i)=-((0.,1.)*OMG*U/topi)*clog(CSQRT((HaL+2*P(i))**2+XaL**2)/
   *SQRT(HaL**2+XaL**2))
      EaR(i)=-((0.,1.)*OMG*U/topi)*clog(CSQRT((HaR+2*P(i))**2+XaR**2)/
   *SQRT(HaR**2+XaR**2))
      EbL(i)=-((0.,1.)*OMG*U/topi)*clog(CSQRT((HbL+2*P(i))**2+XbL**2)/
   *SQRT(HbL**2+XbL**2))
      EbR(i)=-((0.,1.)*OMG*U/topi)*clog(CSQRT((HbR+2*P(i))**2+XbR**2)/
   *SQRT(HbR**2+XbR**2))
      EcL(i)=-((0.,1.)*OMG*U/topi)*clog(CSQRT((HcL+2*P(i))**2+XcL**2)/
   *SQRT(HcL**2+XcL**2))
      EcR(i)=-((0.,1.)*OMG*U/topi)*clog(CSQRT((HcR+2*P(i))**2+XcR**2)/
   *SQRT(HcR**2+XcR**2))

      end do !end of I

C calculations of total electric field for each harmonic

      E(1)=Cur(1)*((EaL(1)+EaR(1))+(EbL(1)+EbR(1))*cos(240.*PI/180.)+
   *  (EcL(1)+EcR(1))*cos(120.*PI/180.))
      E(2)=Cur(2)*((EaL(2)+EaR(2))+(EbL(2)+EbR(2))*cos(120.*PI/180.)+
```

```
     *     (EcL(2)+EcR(2))*cos(240.*PI/180.))
           E(3)=Cur(3)*((EaL(3)+EaR(3))+(EbL(3)+EbR(3))+
     *     (EcL(3)+EcR(3)))

           open(UNIT=20,file='Efield_Harmonics')
           write (20,*) 'Harmonics_E_Field'
           write(20,*) ' Hz   skin-depth    Za      Zph     Eamp      Ephase'

           do i=1,npoint
           K=i*60
           AMPLE(i)=SQRT(REAL(E(i))**2+AIMAG(E(i))**2)
           PhasE(i)=ATAN(AIMAG(E(i))/REAL(E(i)))*180./PI

           write (20,20) k,P(i),Za(i),Zph(i),REAL(E(i)),AIMAG(E(i))
 20        Format (I3,6(2X,F17.10))
           end do
           close(UNIT=20)

C222   continue
       stop
       end

  subroutine layered_Earth(sigma,d,omega,rnu,N,c)
! input parameters
!        sigma(N) - array of layer's conductivity
!        d(N) - layers depth
!        omega - external frequency
!        rnu - wavenumber
!        N - number of layers ( dimension of arrays)
!  output parameters
!        c1 - skin-depth of the 1-st layer
         real d(N),sigma(N)
         complex c(n),alpha2,gamma2,R,gamma
         real pi/3.1415926/
         Rmu0=4.0*pi*1E-7
        gamma2=Rnu*Rnu+(0.,1.)*omega*Rmu0*Sigma(n)
         C(N)=1./SQRT(gamma2)

         do i=N-1,1,-1
          Alpha2=omega*Rmu0*Sigma(i)
          gamma2=Rnu*Rnu+(0.,1.)*Alpha2
          gamma=SQRT(gamma2)
          R=(1.-gamma*C(i+1))/(1.+gamma*C(i+1))
      C(i)=(1.-R*exp(-2.*gamma*d(i)))/gamma/(1.+R*exp(-2.*gamma*d(i)))
         end do

        return
        end
```

7.2 FORTRAN Code 2

```
PROGRAM TO CALCULATE  PSP induced by harmonics
with frequency-dependent pipeline impedances
electric field in the ground induced by harmonics used as the input

      parameter is number of harmonics
      parameter  (nharm=3)
      parameter (Nmax=3000)    !1.E+4)
      real F(nharm),DatEx(nmax,nharm),
     &  DataEy(nmax,nharm),PSP(nmax,nharm), Cur(nmax,nharm)
      COMPLEX Ex(nharm),Ey(nharm),Z,Y, DatZ(nharm),DatY(nharm)
      character*80 fileIN1
      complex ZI(2),V,CI,EAX,EAY, DatP(nharm), DatCurr(nharm)

      real sect(2), fi(2), xx(2)
      common /sections/ nsection, sect, fi,EAX,EAY

      PI=acos(-1.0)
      topi=2.*PI
C     dt=1.E-4  !sampling rate in sec.
      Tmin=1./(60.*nharm)
      dt=Tmin/1000. ! at least 1000 points in the smallest period

C     Nmax=180./(nharm*F*dt) ! maximum size of array for waveform calculations


C electric field for Ontario case
C     EX(1)=1000.*(-3.6E-7,4.9E-3) ! V/km
C     EX(2)=1000.*(-1.25E-8,9.78E-5) !V/km
C     EX(3)=1000.*(-1.08E-2,-4.87E-2) !V/km

C Electric field for Ontario with top water
      EX(1)=1000.*(-0.0000102208,0.0049109999) ! V/km
      EX(2)=1000.*(0.0000000058,0.0000985511) !V/km
      EX(3)=1000.*(-0.0083882259,-0.0189491455) !V/km

C CALCULATIONS OF PSP

C pipeline geometry

      nsection=2 !5

      sect(1)= 250. !115.
      sect(2)=200. !55.
C     sect(3)=30.
C     sect(4)=90.
```

```
C       sect(5)=161.

        fi(1)=1. !3.
        fi(2)=3.   ! 18.
C       fi(3)=55.
C       fi(4)=3.
C       fi(5)=25.

        xx(1)=0.0
        xx(2)=xx(1)
        do i=1,nsection
        xx(2)=xx(2)+sect(i)
        end do

C pipeline terminating impedances
        ZI(1)= (0.1,0.0) !(100.0,0.)
        ZI(2)= (0.1,0.0) !(100.0,0.)
        Np=901
        x=185. !coordinate for PSP calculation


C PSP calculations

    Do i=1,nharm
        F(i)=60.*i
        EAX=EX(i)
        EAY=(0.,0.)   !EY(i) line parallel to pipeline
        OMG=topi*F(i)
        call TLINE(OMG,x,XX,EAX,EAY,ZI,Np,V,CI,Z,Y)
        DatP(i)=V
        DatCurr(i)=CI
        DatZ(i)=Z
        DatY(i)=Y
        end do

C Check the reading
C       open(UNIT=35,file='StartE.dat')
C       do i=1,nharm
C       write(35,35) f(i), EX(i),DatP(i),DatCurr(i)
C 35    Format(7(2X,E15.7))
C       end do
C       goto 110

C conversion of E to time domain (for three fruequency only)

        do i=1,nharm
        F(i)=60.*i
```

```
        DO k=1,Nmax !number of periods for waveform calculations
 !dt=1.E-4 is sampling rate for waveform calculations

        DATEX(k,i)=SQRT((REAL(EX(i)))**2+(AIMAG(EX(i)))**2)*
    &sin(topi*F(i)*dt*k+atan(AIMAG(Ex(i))/REAL(Ex(i))))

C       DATAEY(k,i)=SQRT(REAL(EY(i)**2)+AIMAG(EY(i)**2))*
C    &sin(topi*F(i)*dt*k+atan(AIMAG(EY(i))/REAL(EY(i))))

        PSP(k,i)=SQRT((REAL(DatP(i)))**2+(AIMAG(DatP(i)))**2)*
    &sin(topi*F(i)*dt*k+atan(AIMAG(DatP(i))/REAL(DatP(i))))
        CUR(k,i)=SQRT((REAL(DatCurr(i)))**2+(AIMAG(DatCurr(i)))**2)*
    &sin(topi*F(i)*dt*k+atan(AIMAG(DatCurr(i))/REAL(DatCurr(i))))

        end do

        end do

        open(UNIT=36,file='Pipeline_Impedances.dat')
        do i=1,nharm
        F(i)=60.*i

        write(36,36) F(i), DATZ(i),DATY(i)
 36     Format(5(2X,E15.7))
        end do

C put results in file
        open(UNIT=41,file='Harmonics_psp.dat')
        write (41,*) 'Harmonics_PSP_Current'
C output
        write(41,*) ' sec, dt, F(Hz), Ex (mV/km), PSP(mV), Current(A)'
        do i=1,nharm
        DO k=1,nmax
        write (41,41) k,F(i),DATEx(k,i),PSP(k,i)
    &,Cur(k,i)
 41     Format (I5,4(2X,E15.7))

        end DO

        end do


110     continue

    stop
    end
```

```
      subroutine TLINE(OMG,x,XX,EXA,EYA,ZI,Np,V,CI,Z,Y)

c INPUT PARAMETERS:
c x is coordinate along pipeline where V and CI have to be computed
c XX is a real array of 2 elements: XX(1) beginnig of pipe, XX(2) end of
C pipe
c Z=R+jwL - complex impedance per unit length;
c Y=G+jwC - complex admittance per unit length;
c ZI - complex array of 2 elements: Z(1) terminating impedance at XX(1)
c                                   Z(2) terminating impedance at XX(2)
c Np - number of points for the integration
c OUTPUT PARAMETERS:
c V  - voltage at x
c CI - current at x

      complex Z,Y,ZI(2),V,CI
          complex WNs,ZZ,Zint,Zext,eax,eay
      real x, XX(2),sect(2),fi(2),XXX(2)
      complex Z0,GAMMA,R1,R2,EXA,EYA
      complex K1,K2
      complex P, Q  !  complex integral-function
      complex CNUM1,CNUM2,CDEN
          COMMON /PARAM/ Z0,XXX,GAMMA,N
          common /sections/ nsection, sect, fi,eax,EAy



C   Formulas for Z=int+ext and Y=G+i*OMG*C
C   PIPELINE INPUT VALUES:
C   Rext-external radius of steel,
C   Rint-internal
C   D-coating thickness
C   Cp-conductivity of steelpipe
C   Cs-conductivity of soil
C   Cc-conductivity of coating
C   EPSc-permittvity of the coating
C   Up-magnetic permeability of the steel
C   Us-magnetic permeability of the soil
C   OMG-frequency

          PI=acos(-1.0)
          topi=2.*PI
          XXX(1)=XX(1)
          XXX(2)=XX(2)

C         goto 1
```

```
          Rext=0.457
          Rint=0.448
          D=0.00025  !
          Cp=5.E+6   !
          Cs=1.E-3
          Cc=20.E-6 !coat. conductance per meter^2 change to 20.
          EPSc=3./(18.E+9*topi) ! change to 3.
          Up=150.*(2.*TOPI)/1.E+7  !change to 150
          Us=(2.*TOPI)/1.E+7
          Thk=Rext-Rint
          RR=1./(pi*Cp*(Rext**2-Rint**2))
          Rav=(Rext+Rint)/2.
          WNs=CSQRT((0.0,1.0)*OMG*Us*Cs)  !complex
          ZZ=RR*CSQRT((0.0,1.0)*Up*OMG/topi/thk/RR/Rav)  !complex
          Zint=ZZ*thk*(CEXP(ZZ/RR*thk)+CEXP(-ZZ/RR*thk))/(CEXP(ZZ/RR*thk)
     &    -CEXP(-ZZ/RR*thk))       !complex
          Zext=(0.0,1.0)*OMG*Us/topi*CLOG(2./WNs*Rext)   !complex
          Z=1000.*(Zint+Zext)  !Ohm/km, complex
          G=topi*Cc*(Rext+d)*1.E+3 !S/km
          C=topi*EPSc/(LOG(1.+d/Rext))*1.E+3 !F/km
          Y=(G+(0.0,1.0)*OMG*C) !S/km,complex

1         continue

C         Z=(0.00782,0.00782)
C         Y=(0.00576,0.0)
           N=Np
c define some constants

      Z0=CSQRT(Z/Y)    ! units [ohms]
      GAMMA=CSQRT(Z*Y) ! units [length^-1]
      R1=(ZI(1)-Z0)/(ZI(1)+Z0) ! reflection coef at XX(1)
      R2=(ZI(2)-Z0)/(ZI(2)+Z0) ! reflection coef at XX(2)
      DX=XX(2)-XX(1)

      CNUM1=R2*P(XX(2))*CEXP(-GAMMA*XX(2))
     &-Q(XX(1))*CEXP(GAMMA*XX(2))

      CDEN=CEXP(GAMMA*DX)-R1*R2*CEXP(-GAMMA*DX)

      K1=R1*CEXP(GAMMA*XX(1))*CNUM1/CDEN

      CNUM2=R1*Q(XX(1))*CEXP(GAMMA*XX(1))
     &-P(XX(2))*CEXP(-GAMMA*XX(1))

c denominator is the same CDEN

      K2=R2*CEXP(-GAMMA*XX(2))*CNUM2/CDEN
```

```
 CI=(K1+P(x))*CEXP(-GAMMA*x)
&+(K2+Q(x))*CEXP(GAMMA*x)
 V=Z0*((K1+P(x))*CEXP(-GAMMA*x)
&-(K2+Q(x))*CEXP(GAMMA*x))

 return
 end


 FUNCTION P(x)
 COMMON /PARAM/ Z0,XX,GAMMA,N
      common /sections/ nsection, sect, fi,EAX,EAY
 COMPLEX P,PP,Z0,GAMMA,Epipe,EAX,EAY
 REAL x,XX(2),sect(2),fi(2)

 if(mod(N,2).eq.0) then
   write(*,*) 'mod(N,2)=0 in P'
   stop ' '
 end if

 if(n.le.2) stop ' P: N<=2'

 PP=CEXP(GAMMA*XX(1))*Epipe(XX(1))
 PP=PP+ CEXP(GAMMA*x)*Epipe(x)

 h=(x-XX(1))/(N-1.)

 do i=2,N,2
  xt=XX(1)+h*(i-1)
  PP=PP+ (4.0,0.)*CEXP(GAMMA*xt)*Epipe(xt)
 end do

 do i=3,N-1,2
  xt=XX(1)+h*(i-1)
  PP=PP+ (2.0,0.)*CEXP(GAMMA*xt)*Epipe(xt)
 end do

 P=1./(2.,0.)/Z0*PP*h/3.

 RETURN
 END

 FUNCTION Q(x)
 COMMON /PARAM/ Z0,XX,GAMMA,N
      common /sections/ nsection, sect, fi,EAX,EAY
 COMPLEX Q,QQ,Z0, GAMMA, Epipe,EAX,EAY
 REAL x,XX(2),sect(2),fi(2)
```

```
if(mod(N,2).eq.0) then
  write(*,*) 'mod(N,2)=0 in Q'
  stop ' '
end if

if(n.le.2) stop ' Q: N<=2'

QQ=CEXP(-GAMMA*XX(2))*Epipe(XX(2))
QQ=QQ+ CEXP(-GAMMA*x)*Epipe(x)

h=(XX(2)-x)/(N-1.)

do i=2,N,2
 xt=x+h*(i-1)
 QQ=QQ+(4.0,0.)*CEXP(-GAMMA*xt)*Epipe(xt)
end do

do i=3,N-1,2
 xt=x+h*(i-1)
 QQ=QQ+ (2.0,0.)*CEXP(-GAMMA*xt)*Epipe(xt)
end do

Q=1./(2.0,0.)/Z0*QQ*h/3.

RETURN
END


function Epipe(x)
    common /sections/ nsection, sect, fi,EAX,EAY
complex Epipe,EAX,EAY
real x,sect(2), fi(2)

    RG=3.1415926/180.
    SECTA=SECT(1)
    Epipe=EAY*sin(fi(1)*RG)+EAX*cos(fi(1)*RG)
    Do i=2,nsection
    IF((X-secta).GT.0.0) Epipe=EAY*sin(fi(i)*RG)+EAX*cos(fi(i)*RG)

    SECTA=SECTA+sect(i)
    end do
return
end
```

8. References

Blackburn, J.L., Symmetrical Components for Power Systems Engineering, Marcel Decker, New York, pp 427, 1993.

Boteler, D.H. and Pirjola, R.J., The complex image method for calculating the magnetic and electric fields produced at the surface of the Earth by the auroral electrojet, *Geophys. J. Int*., 132, 31-40, 1998.

Boteler, D.H., Croall, S., Nicholson, P., Measurements of higher harmonics in AC interference on pipelines, Paper #14755, Proceedings CORROSION 2010, NACE, 2010.

Boteler, D.H., Malmborn, K. and Edwall, H.-E., "AC Interference on Pipelines in Southern Sweden", Proceedings of the CEOCOR Symposium, Florence, June 6-7, 2013

Carson, J.R., Wave propagation in overhead wires with ground return, *Bell System Tech. Journal.,* 5, 539,1926.

Dabkowski, J., AC-predictive and mitigation techniques, *Final Report PR-200-9414, PRCI International*, May 1999.

Dawalibi, F.P. and R.D. Southey, Analysis of electrical interference from power lines to gas pipelines. Part I: Computation methods, *IEEE Trans. on Power Delivery*, vol 4, No 3,1840-1846,1989.

Deri, A., G.Tevan, A. Semlyen and A. Castanheira The complex ground-return plane, a simplified model for homogeneous and multi-layer earth return, *IEEE Trans. on Power Apparatus and Systems*, Vol PAS-100, No8, August 1981, pp.3686-3693.

Gary, C. Approche complete de la propagation multifilaire en haute frequence par utilisation des matrices complexes, *EDF Bulletin de la Direction des Etudes et Recherches-Serie B*, No3/4, 1976, pp.5-20

Gummow, R.A., Wakelin, R.G., Segall, S.M., AC Corrosion – A challenge to pipeline integrity, Materials Performance, 38, 2, pp24, February 1999.

Gummow,R., GIC effects on pipeline corrosion and corrosion control system, *Journal of Athmospheric and Solar-Terrestrial Physics*, V 64 No 16 pp. 1755-1764, 2002

Hermance, J.F. & Peltier, W.R., 1970. Magnetotelluric fields of a line current, J. geophys. Res., **75,** 3351–3356.

Kaufman A. A. and G. V. Keller, *The magnetotelluric sounding method (Methods in geochemistry and geophysics; 15)*, pp.187-192, Elsevier Publ. Co., Amst-Oxf.-New York, 1981

Molinski, T.S., Why utilities respect geomagnetically induced currents, J. Atmos. Solar-Terr. Phys., vol 16, no 16, p1765-1778, 2002

Portela, C., J. Gertrudes, M. Tavares and J. Pissolato, Earth conductivity and permittivity measurements : influence on transmission line transient performance, *Electric Power Systems Research*, V. 76, 2006, pp 907-915.

Schelkunoff, S.A., The impedance concept and its application to problems of reflection, refraction, shielding and power absorption, *Bell System Tech. J*., 17, 17, 1938.

Sunde, E.D. *Earth conduction effects in transmission system*, Dover publ., New York, 1968.

Taflove, A. and J. Dabkowski, Prediction method for buried pipeline voltages due to 60 Hz AC inductive coupling, *IEEE Trans. Power Apparatus & Systems*, vol PAS-98, 780-794, 1979.

Trichtchenko, L. and Boteler, D.H., Specification of geomagnetically induced electric fields and currents in pipelines, *J. Geophys. Res*., Vol. 106 , No. A10, 21039-21048, 2001.

Trichtchenko, L. and Boteler, D.H., Effects of Natural Geomagnetic Variations on Power Systems and Pipelines, *Proceedings EMC Conference*, St Petersburg, Sept 2003

Trichtchenko, L., Influence of pipeline electric parameters on AC interference, Paper 14255, Proceedings CORROSION 2010, NACE, Houston, 2010.

Trichtchenko, L., Boteler, D.H., Larocca, P., Modelling the effect of the electromagnetic environment on pipelines, Final Report, PERD Pipeline project 100-7, 2004.

Wagner, C.F. and Evans, R.D., Symmetrical Components: as applied to the analysis of unbalanced electrical circuits, McGraw-Hill, New York, pp 437, 1933.

Wait, J.R., 1992. Electromagnetic Wave Theory, corrected printing, J.R.Wait, Tucson, AZ

Weast, R.C., ed. Handbook of Chemistry and Physics, CRC Press, Inc, 1974.

Weaver, J.T., (1994). *Mathematical Methods for Geo-electromagnetic Induction.* Toronto: John Wiley & Sons Inc